

# Warm Asymmetric Nuclear Matter and Proto-Neutron Star

Pravat Kumar Jena\* and Lambodar Prasad Singh<sup>+</sup>

Department of Physics, Utkal University, Vanivihar,  
Bhubaneswar-751004, India.

## Abstract

Asymmetric nuclear matter equation of state at finite temperature is studied in SU(2) chiral sigma model using mean field approximation. The effect of temperature on effective mass, entropy, and binding energy is discussed. Treating the system as one with two conserved charges the liquid-gas phase transition is investigated. We have also discussed the effect of proton fraction on critical temperature with and without  $\rho$ -meson contribution. We have extended our work to study the structure of proto-neutron star with neutron free charge-neutral matter in beta-equilibrium. We found that the mass and radius of the star decreases as it cools from the entropy per baryon  $S = 2$  to  $S = 0$  and the maximum temperature of the core of the star is about 62 MeV for  $S = 2$ .

PACS Nos: 26.60.+c, 21.30.Fe, 21.60.Jz .

\*email: pkjena@iopb.res.in

<sup>+</sup>email: lambodar@iopb.res.in

# 1 Introduction

The study of properties of hot dense asymmetric nuclear matter has been, in the last few years, vigorously pursued in connection with astrophysical problems[1,2], such as supernova explosions, the evolution of neutron stars and nuclear problems such as heavy-ion-collisions. As the equation of state(EOS) describes the variation of energy density and pressure with density and temperature, it can be used to describe different phases like gaseous and liquid nuclear matter upto the deconfinement transition. It is also possible to study the liquid-gas phase transition, which may occur in the warm and dilute nuclear matter produced in heavy-ion collisions. Several authors using non-relativistic[3] and relativistic[4-8] theories have studied liquid-gas phase transition. Most of the calculations found the critical temperature  $T_c$  lying in the range of 14-20 MeV for symmetric nuclear matter. The critical temperature of symmetric nuclear matter for the most acceptable relativistic Walecka model, is  $T_c \approx 18.3$  MeV[9]. As the asymmetric parameter or the proton fraction plays a vital role in getting the critical temperature, the addition of  $\rho$ -meson is quite essential for the study of asymmetric nuclear matter[4,5].

Field theoretical finite temperature EOS plays an important role in studying the properties and structure of hot dense massive stars such as proto-neutron stars at different temperatures and densities. The important characteristics which determine the composition of matter in a compact star are[10] their relative compressibilities(important to determine maximum mass of neutron star), symmetry energies( important to determine the typical stellar radius and the relative n, p, e, neutrino abundances) and specific heats(important to determine local temperatures). These characteristics vary with respect to the EOS used in different models. Generally the structures of both hot and cold, and both neutron-rich and neutron-poor, stars are fixed by the EOS[2]. A Proto-Neutron Star(PNS) is born following the gravitational collapse of the core of a massive star during a supernova explosion(type-II) and evolves to a cold and deleptonized neutron star, basically through neutrino emission. This very dense and hot core is also able to trap neutrinos, imparting momentum to the outer layers and then

cooling as it reaches a quasi-equilibrium state. There can also be a quark-hadron phase transition in PNS at high density and temperature[11].

In this paper we have extended our earlier study[12] on finite temperature EOS by adding  $\rho$ -meson to the Lagrangian density within the MCH model[13] as the addition of  $\rho$ -meson is quite essential for the study of asymmetric nuclear matter. In our earlier work we have studied the effect of temperature on EOS, effective mass, entropy and binding energy for symmetric nuclear matter and investigated the liquid-gas phase transition using the same model without the  $\rho$ -meson. We now study here how the asymmetric parameter or proton fraction in addition to  $\rho$ -meson changes those properties at finite temperatures. As finite temperature EOS has an important role in studying the structure and properties of astrophysical objects, we have also investigated the structure of PNS taking  $\beta$ -stable charge neutral matter without neutrinos consisting of neutrons, protons and electrons only.

In Sec.2, asymmetric nuclear matter at finite temperature is presented. Proto-neutron star is discussed in Sec.3. We conclude with some remarks in Sec.4.

## 2 Asymmetric nuclear matter at finite temperature

### 2.1 Equation of state

Continuing our earlier investigation [12] on the study of finite temperature effect of asymmetric nuclear matter using MCH model we include here the  $\rho$ -field in the Lagrangian density. The EOS for hadronic phase is calculated by using the Lagrangian density[13] (with  $\hbar = c = K_{Boltzmann} = 1$ ),

$$\begin{aligned} L = & \frac{1}{2}(\partial_\mu \vec{\pi} \cdot \partial^\mu \vec{\pi} + \partial_\mu \sigma \partial^\mu \sigma) - \frac{1}{4}F_{\mu\nu}F_{\mu\nu} - \frac{\lambda}{4}(x^2 - x_0^2)^2 - \frac{\lambda B}{6m^2}(x^2 - x_0^2)^3 \\ & - \frac{\lambda C}{8m^4}(x^2 - x_0^2)^4 - g_\sigma \bar{\psi}(\sigma + i\gamma_5 \vec{\tau} \cdot \vec{\pi})\psi + \bar{\psi}(i\gamma_\mu \partial^\mu - g_\omega \gamma_\mu \omega^\mu)\psi \\ & + \frac{1}{2}g_\omega^2 x^2 \omega_\mu \omega^\mu - \frac{1}{4}G_{\mu\nu} \cdot G^{\mu\nu} + \frac{1}{2}m_\rho^2 \vec{\rho}_\mu \cdot \vec{\rho}^\mu - \frac{1}{2}g_\rho \bar{\psi}(\vec{\rho}_\mu \cdot \vec{\tau} \gamma^\mu)\psi \end{aligned} \quad (1)$$

In the above Lagrangian,  $F_{\mu\nu} \equiv \partial_\mu \omega_\nu - \partial_\nu \omega_\mu$ ,  $G_{\mu\nu} \equiv \partial_\mu \rho_\nu - \partial_\nu \rho_\mu$  and  $x = (\vec{\pi}^2 + \sigma^2)^{1/2}$ ,  $\psi$  is the nucleon isospin doublet,  $\vec{\pi}$  is the pseudoscalar-isovector pion field,  $\sigma$  is the

scalar field and  $\omega_\mu$ , is a dynamically generated isoscalar vector field, which couples to the conserved baryonic current  $j_\mu = \bar{\psi}\gamma_\mu\psi$ .  $\rho_\mu$  is the isotriplet vector meson field with mass  $m_\rho$ . B and C are constant coefficients associated with the higher order self-interactions of the scalar field .

The masses of the nucleon, the scalar meson and the vector meson are respectively given by

$$m = g_\sigma x_0, \quad m_\sigma = \sqrt{2\lambda}x_0, \quad m_\omega = g_\omega x_0 \quad (2)$$

Here  $x_0$  is the vacuum expectation value of the  $\sigma$  field ,  $g_\omega$ ,  $g_\rho$  and  $g_\sigma$  are the coupling constants for the vector and scalar fields respectively and  $\lambda = (m_\sigma^2 - m_\pi^2)/(2f_\pi^2)$ , where  $m_\pi$  is the pion mass ,  $f_\pi$  is the pion decay coupling constant .

Using Mean-field approximation, the equation of motion for isoscalar vector meson field is

$$\omega_0 = \frac{n_B}{g_\omega x^2} \quad (3)$$

and that for  $\rho$ -field is given by

$$\rho_0^3 = (g_\rho/2m_\rho^2)(n_p - n_n) \quad (4)$$

$n_B (= n_p + n_n)$  is the baryon number density at temperature T and is given by

$$n_B = \frac{\gamma}{(2\pi)^3} \int_0^\infty d^3k [n_i(T) - \bar{n}_i(T)] \quad (5)$$

with

$$n_i(T) = \frac{1}{e^{(E^*(k)-\nu_i)\beta} + 1}, \quad (6)$$

$$\bar{n}_i(T) = \frac{1}{e^{(E^*(k)+\nu_i)\beta} + 1}, \quad (7)$$

where  $i = n, p$ .  $E^*(k) = (k^2 + y^2m^2)^{1/2}$  is the effective nucleon energy,  $\beta = 1/K_B T$ ,  $\gamma$  is the spin degeneracy factor with  $n_i(T)$  and  $\bar{n}_i(T)$  being Fermi-Dirac distribution functions for particle and anti-particle respectively at finite temperature.  $\nu_i$  is the effective baryon chemical potential which is related to the chemical potential  $\mu_i$  as

$$\nu_p = \mu_p - \frac{C_\omega n_B}{y^2} - \frac{C_\rho}{4}(n_p - n_n) \quad (8)$$

$$\nu_n = \mu_n - \frac{C_\omega n_B}{y^2} + \frac{C_\rho}{4}(n_p - n_n) \quad (9)$$

and  $y \equiv x/x_0$  is the effective mass factor which must be determined self consistently from the equation of motion for scalar field which is given by

$$(1-y^2) - \frac{B}{m^2 C_\omega} (1-y^2)^2 + \frac{C}{m^4 C_\omega^2} (1-y^2)^3 + \frac{2C_\sigma C_\omega n_B^2}{m^2 y^4} - \frac{C_\sigma \gamma}{\pi^2} \int_0^\infty \frac{dk k^2 (n_i(T) + \bar{n}_i(T))}{\sqrt{k^2 + m^{*2}}} = 0. \quad (10)$$

$m^* \equiv ym$  is the effective mass of the nucleon and the coupling constants are

$$C_\sigma \equiv \frac{g_\sigma^2}{m_\sigma^2}, \quad C_\omega \equiv \frac{g_\omega^2}{m_\omega^2} \quad \text{and} \quad C_\rho \equiv g_\rho^2/m_\rho^2. \quad (11)$$

The symmetric energy coefficient that follows from the semi-empirical nuclear mass formula is[13]  $a_{sym} = \frac{C_\rho k_f^3}{12\pi^2} + \frac{k_f^2}{6\sqrt{k_f^2 + m^{*2}}}.$

Now the nucleon number densities, energy density and pressure at finite temperature and finite density are given by

$$n_p = \frac{\gamma}{(2\pi)^3} \int_0^\infty d^3k [n_p(T) - \bar{n}_p(T)] \quad (12)$$

$$n_n = \frac{\gamma}{(2\pi)^3} \int_0^\infty d^3k [n_n(T) - \bar{n}_n(T)] \quad (13)$$

$$\begin{aligned} \epsilon = & \frac{m^2(1-y^2)^2}{8C_\sigma} - \frac{B}{12C_\omega C_\sigma} (1-y^2)^3 + \frac{C}{16m^2 C_\omega^2 C_\sigma} (1-y^2)^4 + \frac{C_\omega n_B^2}{2y^2} + \frac{1}{2} m_\rho^2 (\rho_0^3)^2 \\ & + \frac{\gamma}{2\pi^2} \int_0^\infty dk k^2 \sqrt{(k^2 + m^{*2})} [n_n(T) + \bar{n}_n(T) + n_p(T) + \bar{n}_p(T)] \end{aligned} \quad (14)$$

$$\begin{aligned} P = & -\frac{m^2(1-y^2)^2}{8C_\sigma} + \frac{B}{12C_\omega C_\sigma} (1-y^2)^3 - \frac{C}{16m^2 C_\omega^2 C_\sigma} (1-y^2)^4 + \frac{C_\omega n_B^2}{2y^2} \\ & + \frac{1}{2} m_\rho^2 (\rho_0^3)^2 + \frac{\gamma}{6\pi^2} \int_0^\infty \frac{dk k^4 [n_n(T) + \bar{n}_n(T) + n_p(T) + \bar{n}_p(T)]}{\sqrt{(k^2 + m^{*2})}} \end{aligned} \quad (15)$$

The entropy density(S/V) and entropy per baryon(S) can be obtained as

$$S/V = (P + \epsilon - \mu_p n_p - \mu_n n_n) \beta \quad (16)$$

$$S = (P + \epsilon - \mu_p n_p - \mu_n n_n) \beta / n_B \quad (17)$$

In order to describe the asymmetric nuclear matter one can introduce the proton fraction which is defined as

$$y_p = \frac{n_p}{n_B} \quad (18)$$

For the neutron matter  $y_p = 0$  and for symmetric nuclear matter  $y_p = 0.5$ .

The values of four parameters  $C_\sigma, C_\omega, C_\rho, B$  and  $C$  occurring in the above equations are obtained[13] by fitting with the saturation values of binding energy/nucleon(-16.3 MeV), the saturation density( $0.153 \text{ fm}^{-3}$ ), the symmetric energy(32 MeV), the effective(Landau) mass(0.85 M), and nuclear incompressibility( $\sim 300 \text{ MeV}$ ), are  $C_\omega = 1.999 \text{ fm}^2$ ,  $C_\sigma = 6.816 \text{ fm}^2$ ,  $C_\rho = 4.661 \text{ fm}^2$ ,  $B = -99.985$  and  $C = -132.246$ . For a given value of  $n_B$  at fixed  $y_p$  and/or T, the equations[10,12,13] can be solved self-consistently to get  $y$ ,  $\mu_p$ ,  $\mu_n$  and making substitution, the energy density, pressure, entropy density and entropy per baryon can be evaluated.

Now let us discuss the liquid-gas phase transition. In case of the more common single component phase equilibria, such as liquid vapour, the phases are distinguished by only one parameter, e.g. the density whereas the binary mixture has the additional parameter, the proton fraction  $y_p$ , which is different from one phase to the other[14]. For the description of liquid-gas phase transition we have followed here the thermodynamic approach of Refs.[7,14,15]. In the case of asymmetric nuclear matter the system is characterized by two conserved charges namely the baryon density( $n_B = n_p + n_n$ ) and the total charge or equivalently the third component of isospin( $I_3 = \frac{n_p - n_n}{2}$ ) or equivalently the proton fraction( $y_p$ ). Thus the stability criteria may be expressed by the following relations[7]

$$n_B \left( \frac{\partial P}{\partial n_B} \right)_{T,y_p} > 0 \quad (19)$$

$$\left( \frac{\partial \mu_p}{\partial y_p} \right)_{T,P} > 0, \quad \text{or} \quad \left( \frac{\partial \mu_n}{\partial y_p} \right)_{T,P} < 0 \quad (20)$$

The first inequality shows that isothermal compressibility is positive which implies that the system is mechanically stable. The second condition expresses the diffusive stability. If any of the three stability criteria is violated then there will be a phase separation[7].

## 2.2 Results and discussions

First, we discuss the effective nucleon mass of nuclear matter at finite temperature and density. Fig.1 shows the effective mass versus number density at temperatures  $T=0, 100, 200$  MeV. The solid lines are for  $y_p = 0.5$  and dotted lines are for  $y_p = 0$ . It is observed that in all temperatures  $M^*$  decreases with the increase of  $n_B$ . For  $T=0$  or  $T=100$  MeV, the effective mass varies little with  $y_p$ , whereas it is very sensitive with  $y_p$  for  $T=200$  MeV. It is also clear that at zero density, the effective mass is the same for neutron matter and symmetric matter at different temperature. Hence these result indicate that the nucleons of neutron matter must stay in higher energy levels compared to that of symmetric matter in order to have the same number density and the difference will decrease as the number density decreases. This result agrees with that obtained in Ref.6.

In Fig.2 we show the effective mass as a function temperature at zero density( $n_B = 0$ ) and saturation density( $n_B = 0.153\text{fm}^{-3}$ ). The solid lines are for symmetric nuclear matter( $y_p=0.5$ ) and dotted lines for neutron matter( $y_p = 0$ ). It is clear from figure that for  $n_B = 0$ , the solid line and the dotted line are same, whereas for  $n_B = n_0$ , the  $y_p$  dependence is sensitive to the temperature in between 150 MeV and 240 MeV and again the two lines coincide at higher temperatures. It is also observed that for  $n_B = n_0$ , the  $M^*$  first increases slowly and then falls suddenly at about  $T \approx 240$  MeV. But for  $n_B = 0$ ,  $M^*$  remains almost constant as the temperature increases and falls suddenly at about  $T \approx 235$  MeV. This result shows that a first order phase transition appears at  $n_B = 0$ ,  $T \approx 235$  MeV which is similar to the result obtained for Walecka model, which has such a phase transition at  $T \approx 185$  MeV[16]. Because of strong attraction between the nucleons at high temperatures the nucleon antinucleon pairs can be formed which may lead to abrupt change in  $M^*$  to take place in high temperature region. But the mechanism of this first order phase transition is not clear. It is expected that this abrupt change of  $M^*$  in the high temperature region for some models including the Walecka model might be related to the formation of new matter[17].

Fig.3 shows the binding energy per nucleon as a function of the baryon density at

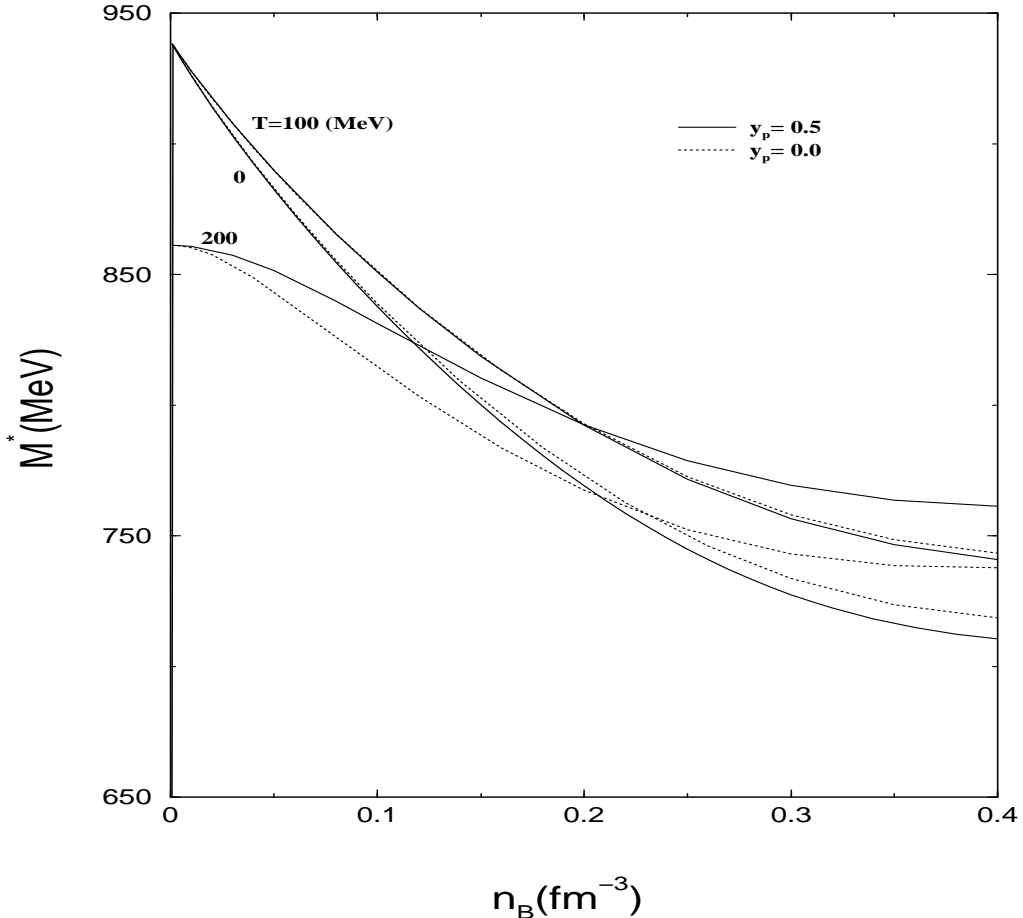


Figure 1: *Effective mass as function of baryon number density at different temperatures.*

different temperatures for symmetric nuclear matter,  $y_p=0.5$ . At zero temperature it has a minimum at the nuclear saturation density  $n_0$  which corresponds to a binding energy per nucleon of -16.3 MeV. With the increase of temperature the minimum shifts towards higher densities and for higher temperatures the minimum of the curve becomes positive. It is also observed that as the temperature increases, the nuclear matter becomes less bound and the saturation curves in the MCH model are seems to be flatter than those observed in Walecka model[17,18]. This result implies that the nuclear matter EOS in MCH model is softer than that obtained in Walecka model.

In Fig.4, we show pressure as a function of density  $n_B$  at different temperatures. The solid lines are for symmetric nuclear matter and the dotted are for pure neutron matter which are stiffer at all temperatures. For a given  $n_B$ , the pressure has the

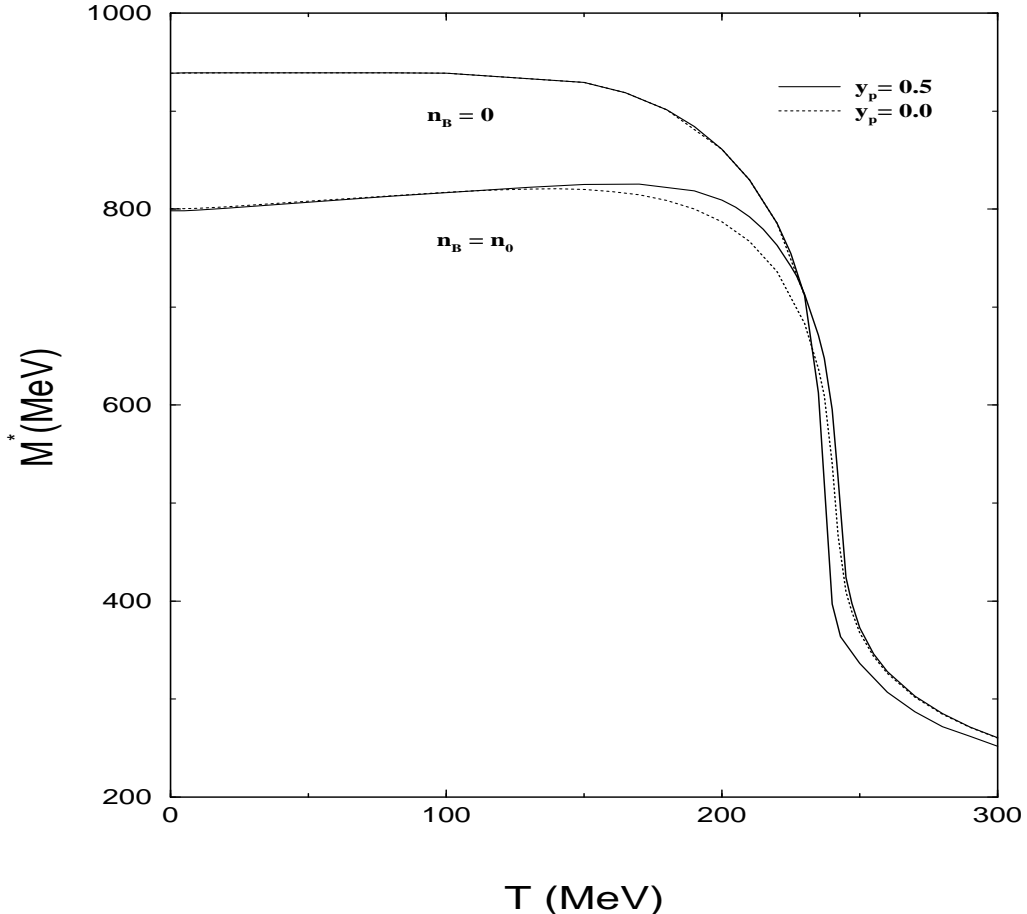


Figure 2: *Effective mass as function of temperature for constant baryon number densities.*

usual trend of increasing with temperature[19]. As the temperature increases the EOS becomes stiffer. Pressure has a non-zero value for  $n_B = 0$  at and above a temperature of 200 MeV. It indicates that pressure has a contribution arising from the thermal distribution functions for baryons and anti-baryons as well as from the non-zero value of the scalar field. Similar results were also obtained by Panda *et al.*[20] for symmetric nuclear matter. The non-zero value for scalar  $\sigma$  field has also been observed in Walecka model[19].

The entropy density as a function of density at different temperatures for symmetric nuclear matter and pure neutron matter is presented in Fig.5. It is observed that entropy density for both is non-zero even at vanishing baryon density at a temperature

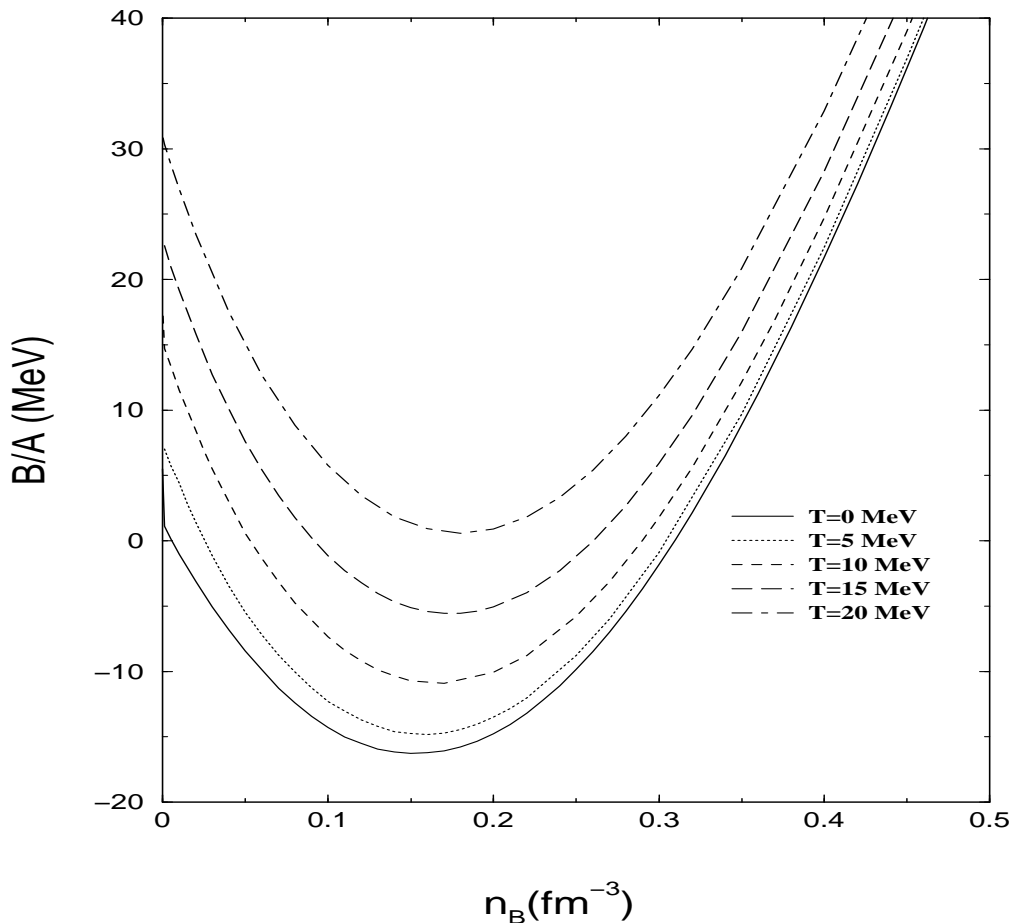


Figure 3: *Binding energy per nucleon as function of baryon number density at different temperatures.*

of 200 MeV with contributions from the non-zero value of the sigma field. Similar behavior was also observed for entropy density in the Walecka model and ZM model calculations[18]. This increase of entropy density with increase of temperature indicates a phase transition. The Entropy per baryon( $S$ ) as a function of baryon number density at different temperatures for symmetric nuclear matter is shown in Fig.6. At lower temperatures  $S$  decreases slowly as compared to higher temperatures and the minimum value of  $S$  increases as the temperature increases which is similar to the result obtained in Refs.[2,8].

We now discuss the liquid-gas phase transition. The pressure as a function of baryon density at fixed temperature  $T = 10$  MeV with different proton fractions is shown in

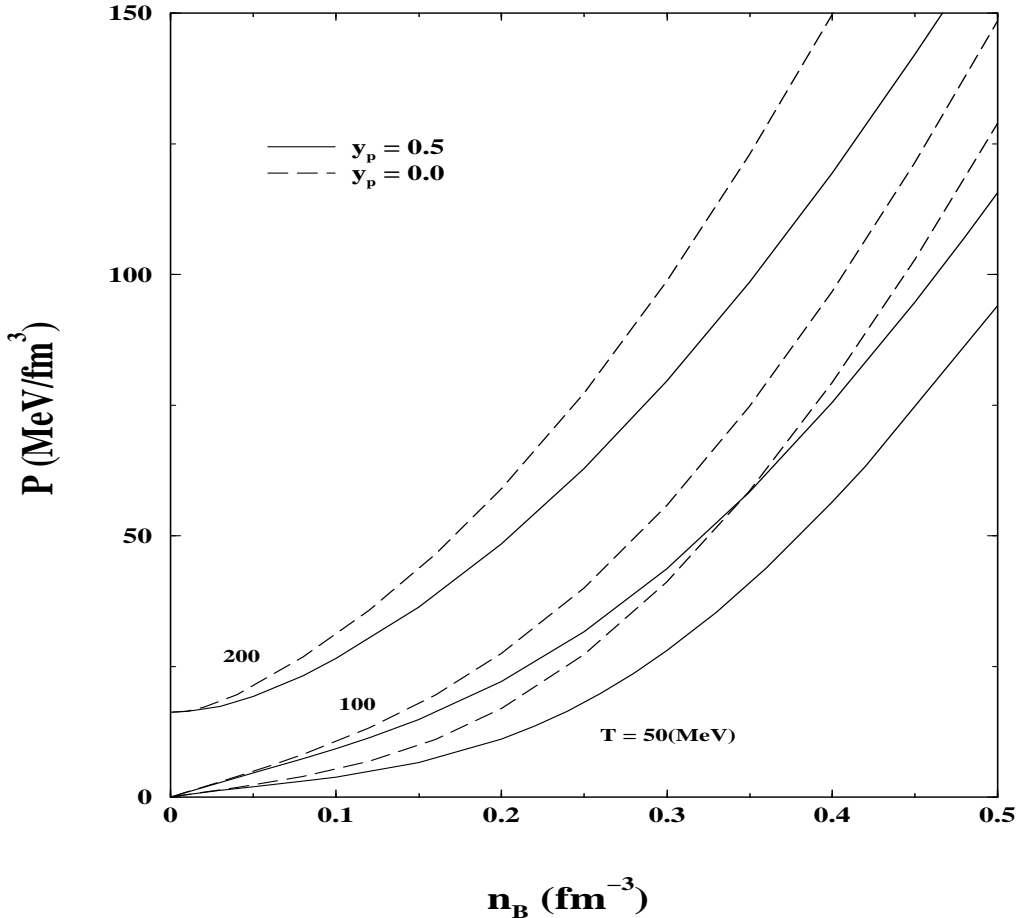


Figure 4: Pressure ( $P$ ) as function of baryon number density at different temperatures.

Fig.7. It may be observed from the figure that for any fixed density with fixed  $T = 10$  MeV, the pressure is not constant rather it increases with decrease of proton fraction. This clearly indicates that for asymmetric nuclear matter during isotherm liquid-gas phase transition the pressure can not remain constant but increases monotonically. It shows that for small  $y_p$ , particularly for neutron matter( $y_p=0$ ), the pressure increases monotonically which indicates that matter is stable at all densities. But for  $y_p \geq 0.2$ , the compressibility becomes negative, indicating mechanical instability. The diffusive unstable regions can be seen clearly from Fig.8, where the chemical potentials of proton and neutron is shown as a function of  $y_p$  at fixed pressure  $P = 0.1$  MeV/fm<sup>3</sup> and temperature  $T = 10$  MeV. According to the inequality[20] the region of negative slope for  $\mu_p$  and positive slope for  $\mu_n$  is unstable. Thus violation of stability criteria is an

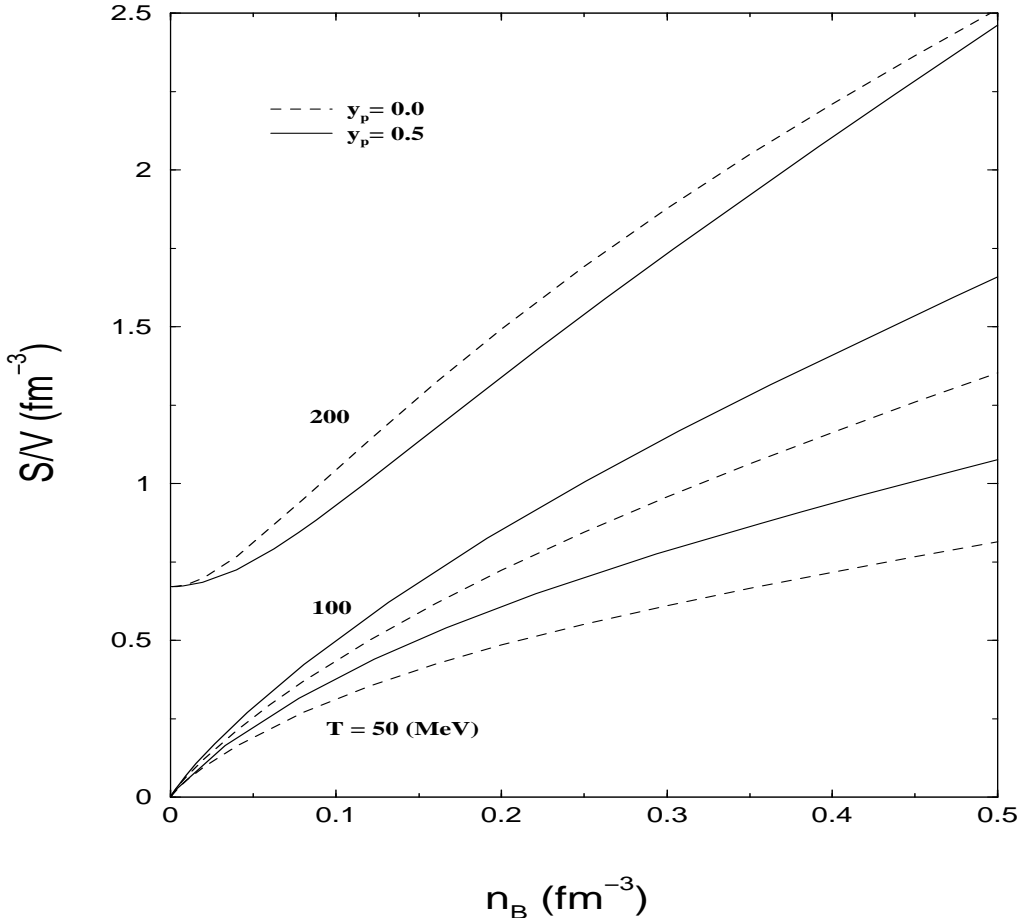


Figure 5: *Entropy density as function of baryon number density at different temperatures.*

indication of phase separation.

Fig.9 shows the variation of pressure as a function of baryon density for different  $y_p$ . One can see that the region of mechanical instability decreases both with increase of temperature and decrease of proton fraction[8]. We present the pressure of symmetric nuclear matter as a function of baryon density for low temperatures in Fig.10. The figure shows that at zero temperature, the pressure first decreases, then increases and passes through  $P = 0$  at  $n_B = n_0$  (saturation density), where the binding energy per nucleon is a minimum. Decrease of pressure with density implies a negative incompressibility,  $K = 9(\frac{\partial P}{\partial n_B})$ , which is a sign of mechanical instability. When the temperature increases the region of mechanical instability decreases and disappears

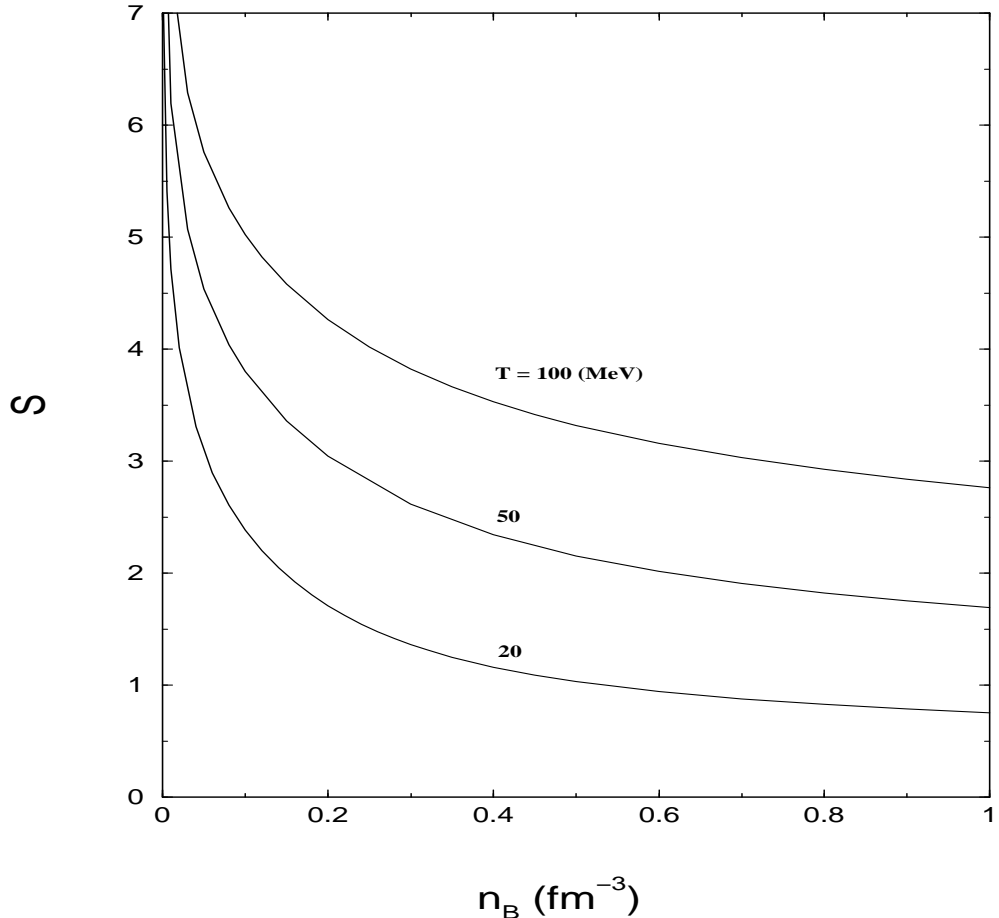


Figure 6: *Entropy per baryon as a function of baryon number density at different temperatures.*

at the critical temperature  $T_c$ , which is determined by  $\frac{\partial P}{\partial n_B} \Big|_{T_c} = \frac{\partial^2 P}{\partial^2 n_B} \Big|_{T_c} = 0$ , above which the liquid-gas phase transition is continuous. We have obtained the value of critical temperature  $T_c \approx 17.2 \text{ MeV}$ , critical density  $n_c \approx 0.045 \text{ fm}^{-3}$ , critical pressure  $p_c \approx 0.274 \text{ MeV/fm}^{-3}$  and critical effective mass  $M_c^* \approx 887 \text{ MeV}$  which is in fair agreement with the results obtained in other studies[8,17,18].

In Fig.11, we plot the variation of critical temperature with different proton fraction( $y_p$ ) with and without  $\rho$ . The critical temperature  $T_c$  decreases monotonically[8,21] as the proton fraction decreases and goes to zero for  $y_p = 0.02$  with  $\rho$  whereas  $T_c = 11.6$  at  $y_p = 0$  without  $\rho$ . This indicates that addition of  $\rho$ -meson lowers the critical temperature at smaller  $y_p$ . As may be seen from equations[8,9], the addition of  $\rho$ -meson gives a

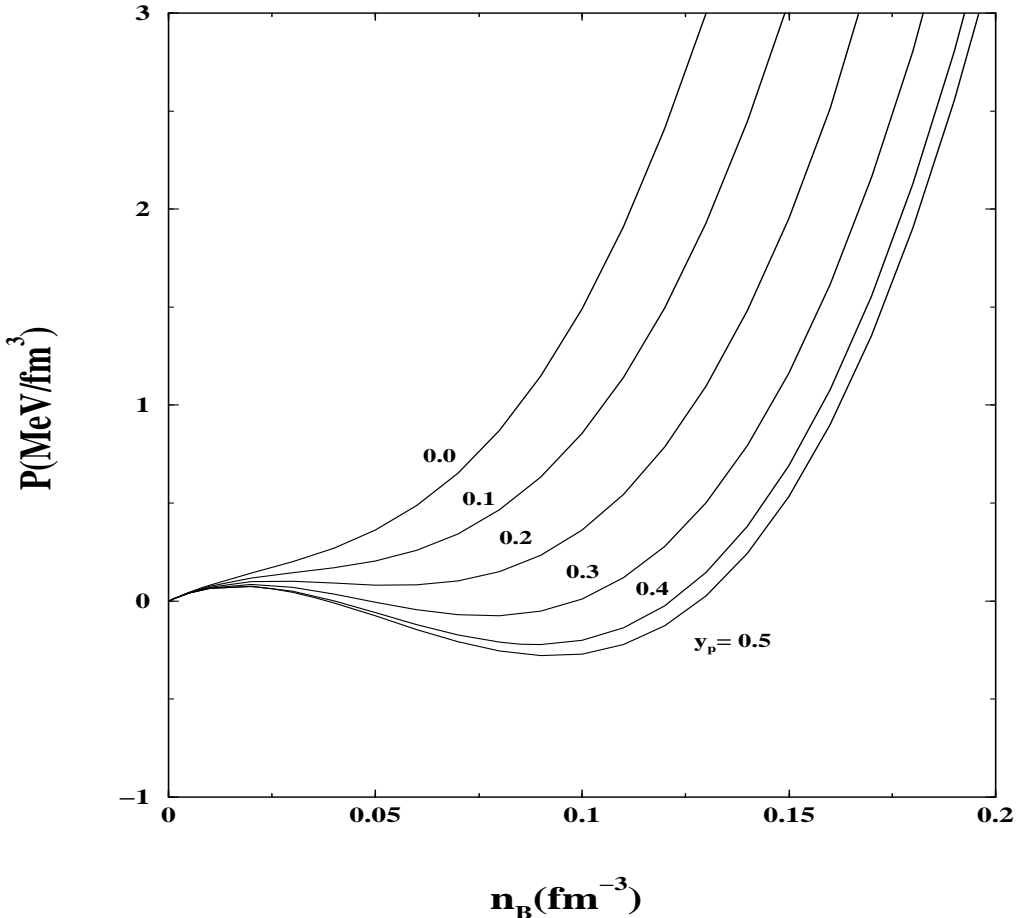


Figure 7: Pressure as a function of baryon number density for different proton fractions at temperature  $T=10$  MeV.

repulsive potential which makes the nuclear matter easier to be gasified. But for neutron matter( $y_p = 0$ ), the system only remain in gas phase even at zero temperature[6].

### 3 Proto-Neutron Star

In this section we extend our investigation to a study of the structure and properties of Proto-Neutron Star. A PNS is born following the gravitational collapse of the core of a massive star during a Supernova explosion(type-II). It is a hot collapsed core which can reach temperatures as high as few tens of MeV. The evolution of PNS proceeding

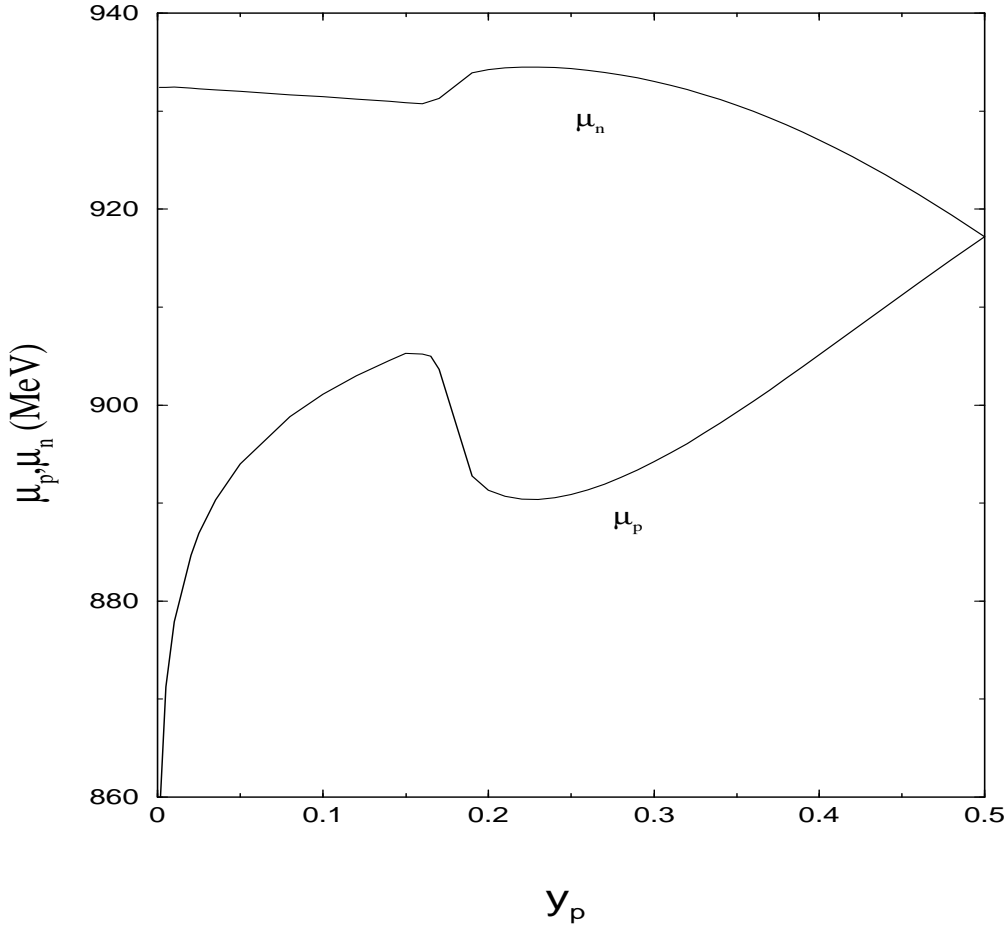


Figure 8: *Chemical potentials as a function of  $y_p$  at temperature  $T=10$  MeV and  $P=0.1$  MeV/fm $^3$*

through several distinct states with various outcomes is discussed in Ref.[2]. During the early evolution of PNS, a neutron star with an entropy per baryon of order of unity contains neutrinos that are trapped in matter on dynamical time scale and after a lapse of few tens of seconds the star achieves it's cold catalysed structure with essentially zero temperature and zero trapped neutrinos. A PNS has approximately uniform entropy per baryon(S) of 1-2 across the star[22]. At birth the PNS has S=1. After deleptonization the entropy per baryon reaches its maximum (S $\sim$  2) and finally cools down to its cold state with S=0[2]. The finite temperature aspect of EOS plays an important role in the study of properties and structure of PNS.

The structure of PNS mainly depends on it's composition[2]. Since the composition

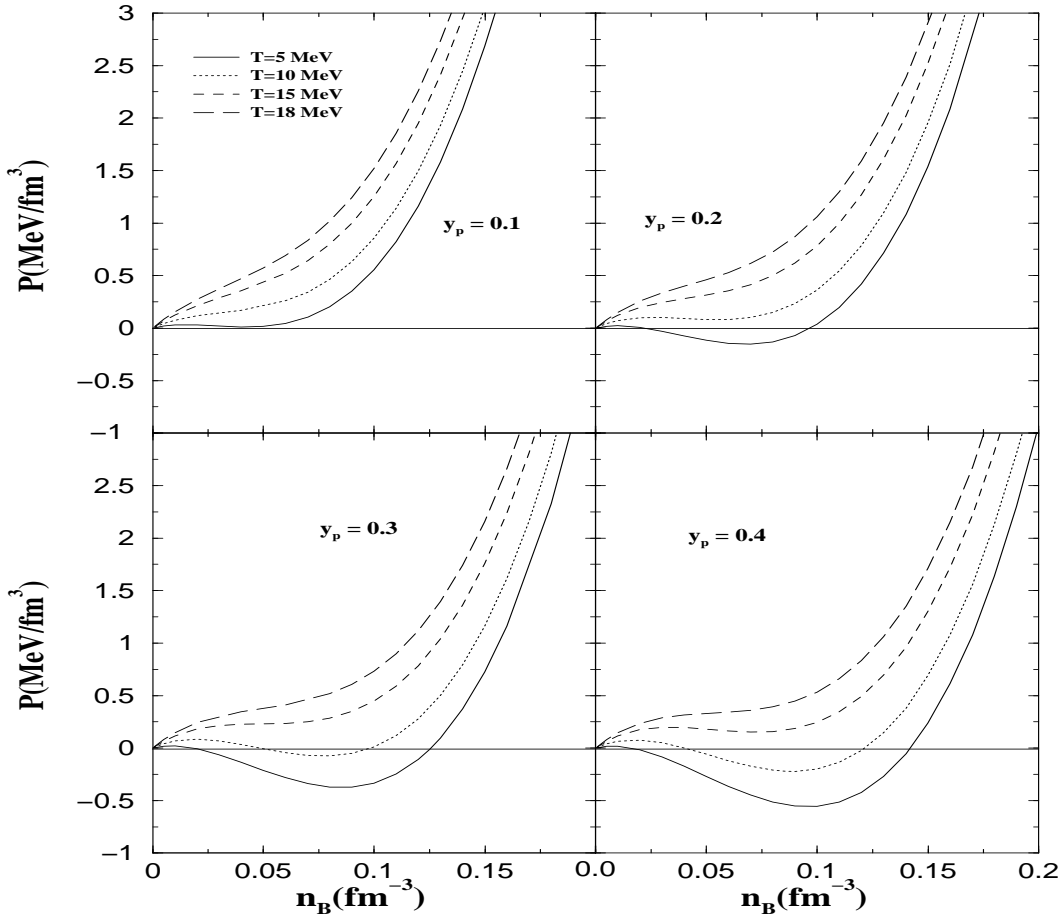


Figure 9: Pressure as a function of baryon number density for different proton fractions

of neutron star basically depends on the nature of strong interactions which are not well understood in dense matter, one has to investigate various possible conditions taking many possible models. Out of various possible cases discussed in Ref.[2], we consider here a case in which matter consists of neutrons, protons and electrons whose relative concentrations is determined from the conditions of charge neutrality and  $\beta$ -equilibrium in the absence of neutrino trapping[2].

The  $\beta$ -equilibrium (without neutrino trapping) and the charge neutrality conditions are respectively given by

$$\mu_n = \mu_p + \mu_e \quad (21)$$

and

$$n_p = n_e \quad (22)$$

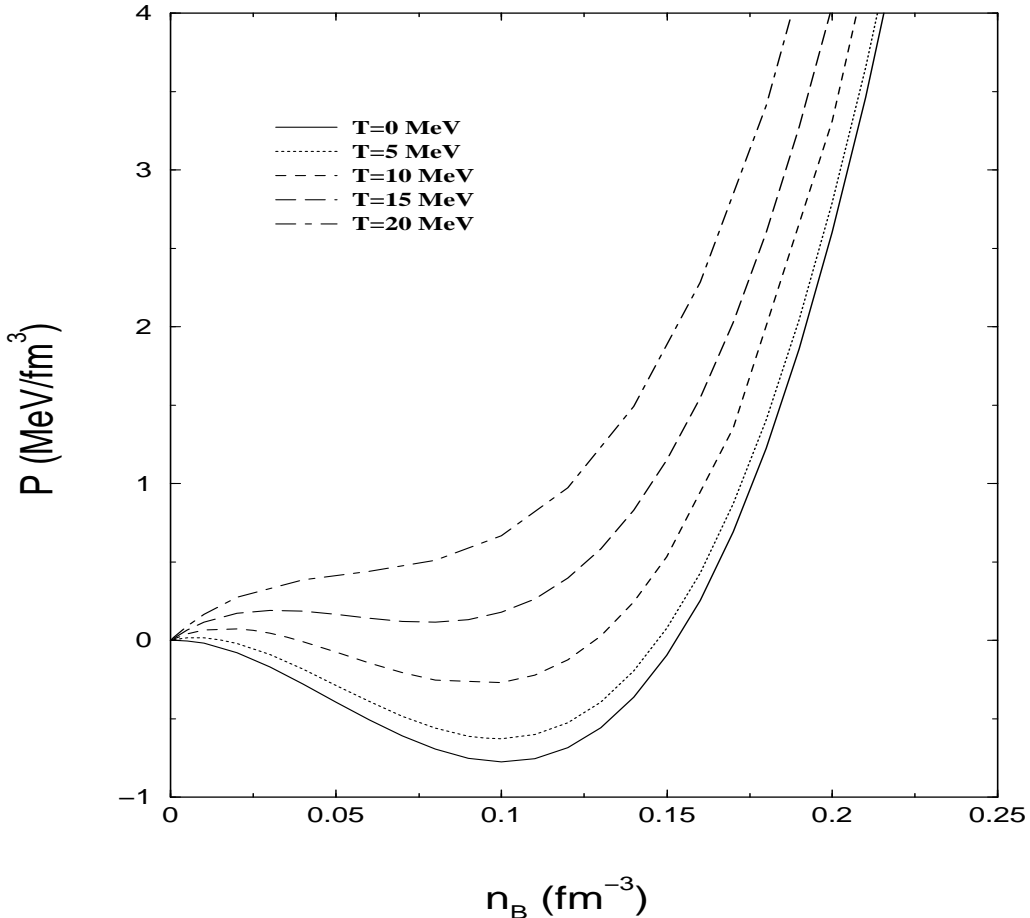


Figure 10: Pressure ( $P$ ) as function of baryon number density for symmetric matter at different temperatures.

Where  $\mu_e$  and  $n_e$  are chemical potentials and number density of electron respectively.

The electron number density at finite temperature can be written as

$$n_e = \frac{\gamma}{(2\pi)^3} \int_0^\infty d^3k [n_e(T) - \bar{n}_e(T)] \quad (23)$$

Where

$$n_e(T) = \frac{1}{e^{(\sqrt{(k^2+m_e^2)}-\mu_e)\beta} + 1}, \quad \bar{n}_e(T) = \frac{1}{e^{(\sqrt{(k^2+m_e^2)}+\mu_e)\beta} + 1}, \quad (24)$$

The number density of neutron and proton is defined in Eqns.12 and 13. The extra terms which must be added to energy density and pressure (given in eqns. 14 and 15)

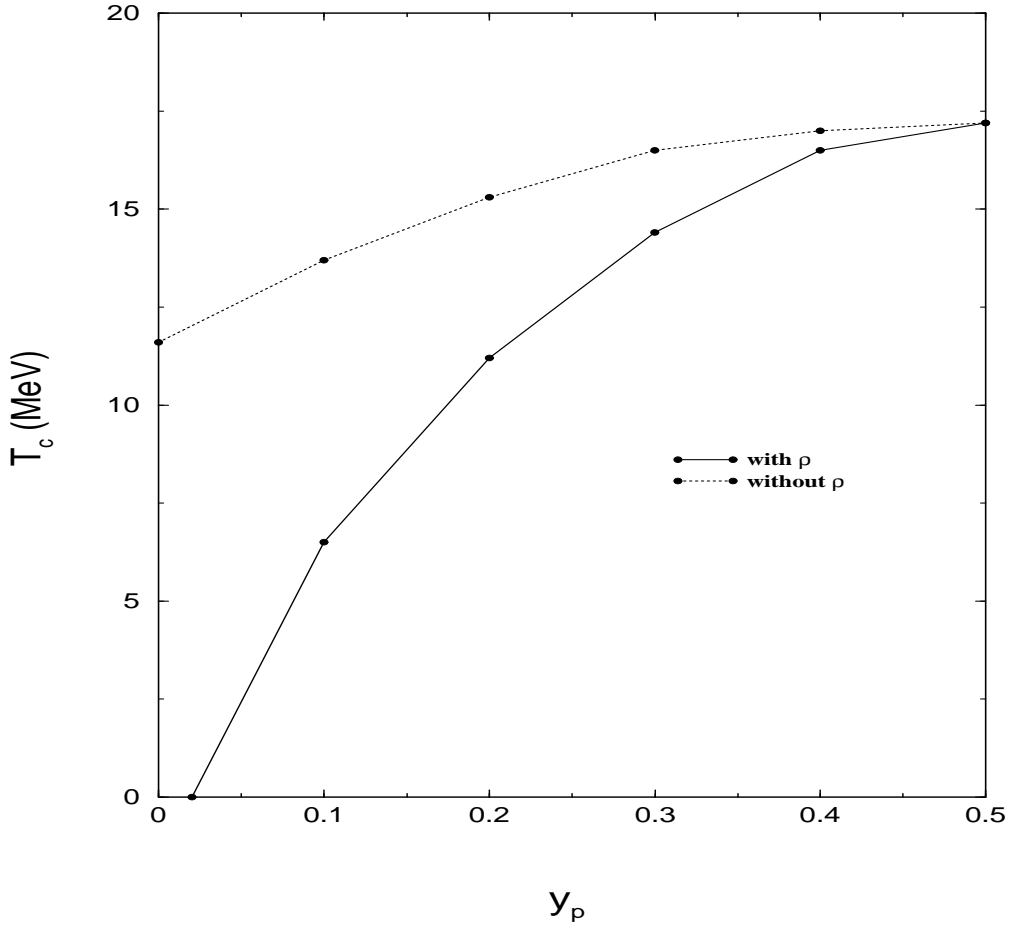


Figure 11: *Critical temperature versus proton fraction  $y_p$ .*

are respectively

$$\frac{\gamma}{2\pi^2} \int_0^\infty dk k^2 \sqrt{(k^2 + m_e^2)} [n_e(T) + \bar{n}_e(T)] \quad (25)$$

and

$$\frac{\gamma}{6\pi^2} \int_0^\infty \frac{dk k^4 [n_e(T) + \bar{n}_e(T)]}{\sqrt{(k^2 + m_e^2)}} \quad (26)$$

For a given value of  $n_B$ , the equations[10,12,13,17,23] are to be solved self-consistently using Eqns.19 and 20 (for fixed  $S=0,1$  or 2) to get  $\mu_p, \mu_e, n_p, y, T$  and then can be substituted to get pressure and energy density. After getting pressure as function of energy density, the TOV equations can be integrated using proper boundary conditions[13] to get mass and radius of star at fixed entropy per baryon  $S$ .

Pressure as a function of number density for  $S = 0, 1$  and  $2$  is shown in Fig.12.

One can mark from the figure that the EOS becomes softer as the entropy per baryon decreases from  $S=2$  to  $S=0$  which indicates the lowering of mass and radius as shown in Fig.13 and Fig.14 respectively. For different values of  $S$ , the radius, energy density, pressure, number density and temperature corresponding to maximum mass is given in the following table.

**Table**

Star properties for matter in beta-equilibrium at finite entropy.

S	$\frac{M_{max}}{M_\odot}$	R (km)	$\epsilon_c$ ( $\frac{MeV}{fm^3}$ )	$n_c$ ( $fm^{-3}$ )	$P_c$ ( $\frac{MeV}{fm^3}$ )	$T_c$ (MeV)
0	2.18	12.14	1230	0.97	304.71	0.0
1	2.21	12.23	1190	0.94	294.85	27.85
2	2.33	12.45	1092	0.85	272.24	62.12

The results in the table reflects the influence of entropy on the gross properties of stars. Increase of maximum mass and radius upto  $S=2$ , amounts to only a few percent of cold star and the temperature of the core is upto 62 MeV which is in fair agreement with the results obtained in Ref.[2]. It also shows that for  $S=2$ , the thermal contribution is larger which results in an increase of mass of about  $0.15 M_\odot$  compared with that for  $S=0$ . In neutron stars, the pressure is supported by strongly interacting baryons which have smaller contributions to the pressure which causes a smaller increase in maximum mass. Thus the compositional variable of EOS has more importance than the temperature for the structure of neutron star[2]. But for a White Dwarf which have highly ideal EOS[23], the structure and properties are very sensitivity to the entropy per baryon.

The relative concentrations of chemical potentials of  $n, p$  and  $e$  in beta-equilibrium at a fixed entropy per baryon  $S=1$ , is shown in Fig.15. It is clear that  $\mu_e$  increases linearly with number density whereas  $\mu_n$  and  $\mu_p$  first decreases and then increases linearly. The increase of electron chemical potential with number density implies the abundance of

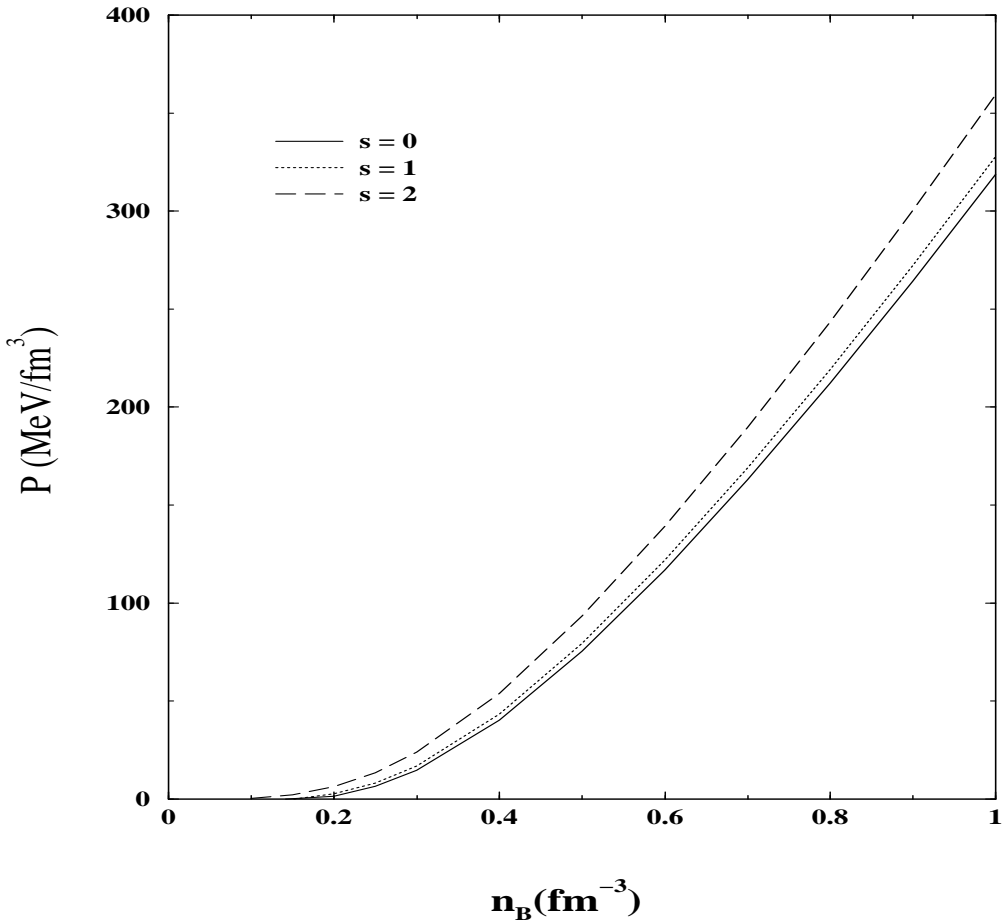


Figure 12: *Pressure as a function of number density at fixed entropy per baryon.*

negatively charged particle(electron) which shows that the system is proton rich over an extended region of density. It may be seen from the figure that in the very lower density region the proton abundance is more, then decreases to some extent and then increases linearly in high density region.

The temperature as a function of energy density at fixed entropy per baryon is shown in Fig.16. The temperature of the star increases for both  $S=1$  and  $S=2$  from which one can get the critical temperature corresponding to the maximum mass of the star. The temperature is maximum at the center of the star (where central energy density is about 1100-1200 MeV/fm<sup>3</sup> for a maximum mass star) and decreases with decreasing energy density which is faster particularly at lower energy densities. This implies that the interior of the star maintains a small variation of temperature but falls

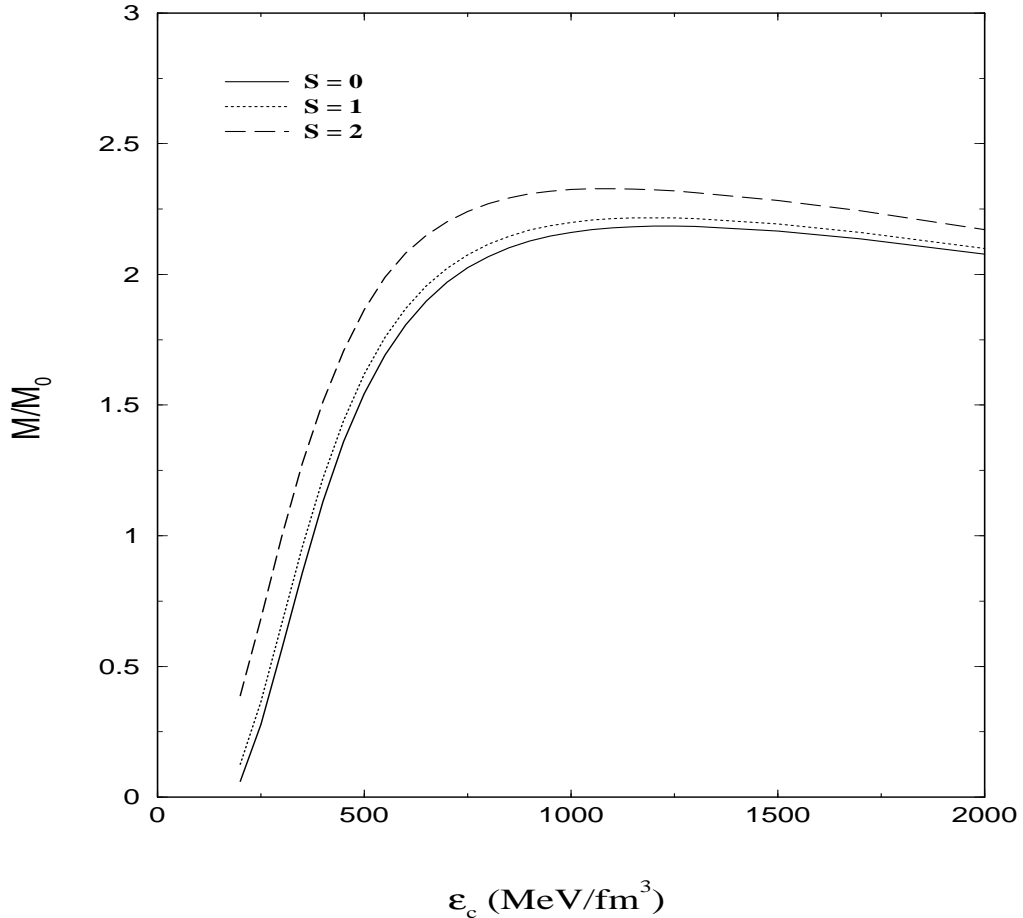


Figure 13: *Star mass ( $M/M_\odot$ ) as a function of central energy density at fixed entropy per baryon.*

rapidly towards the surface region as density decreases.

## 4 Conclusions

We have studied here asymmetric nuclear matter at finite temperature using the MCH model[13]. We have presented how the effective nucleon mass, energy per baryon, entropy density, entropy per baryon and pressure behave as a function of density for various temperatures. At zero density we find that this model exhibit a phase transition at  $T \approx 235$  MeV just as obtained in the Walecka model at  $T \approx 185$  MeV. This model exhibits the existence of liquid-gas phase transition in asymmetric nuclear matter and

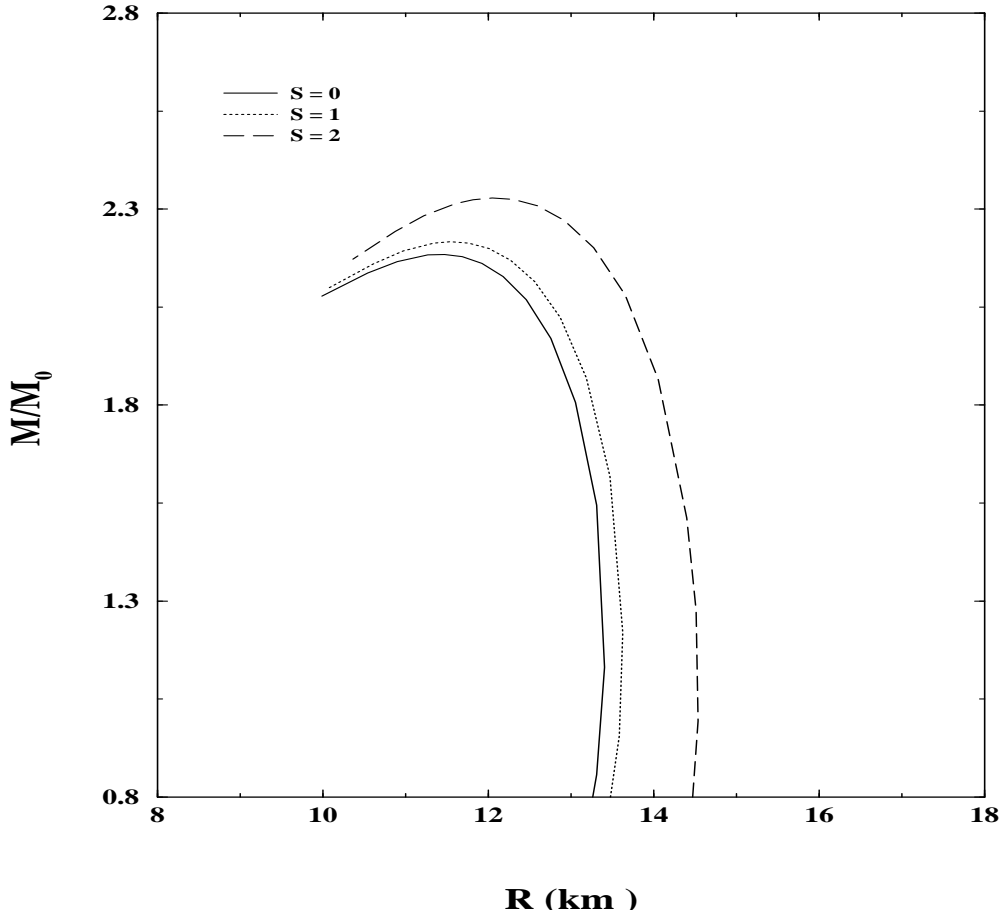


Figure 14: *Radius versus star mass at fixed entropy per baryon.*

the critical temperature  $T_c$  depends sensitively on the proton fraction  $y_p$ .  $T_c$  decreases with the decrease of  $y_p$  as shown in Fig.11. The value of critical temperature decreases from  $T_c \approx 17.2$  to 11.6 MeV for  $y_p = 0.5$  to 0 without  $\rho$ -meson and from  $T_c \approx 17.2$  to 0 MeV for  $y_p = 0.5$  to 0.02 with  $\rho$ -meson. Hence the addition of  $\rho$ -meson seems to be very important to the study of properties of asymmetric nuclear matter as it lowers the critical temperature. This also shows that even at zero temperature the system remain only in gas phase for neutron matter( $y_p = 0$ ). At fixed temperature and density the pressure of the system increases with decrease of proton fraction(shown in Fig.7) which indicates that during the isotherm liquid-gas phase transition pressure can not remain constant for asymmetric nuclear matter. We have also studied the EOS and structure of PNS with neutrino free charge neutral matter in beta-equilibrium. We find that as

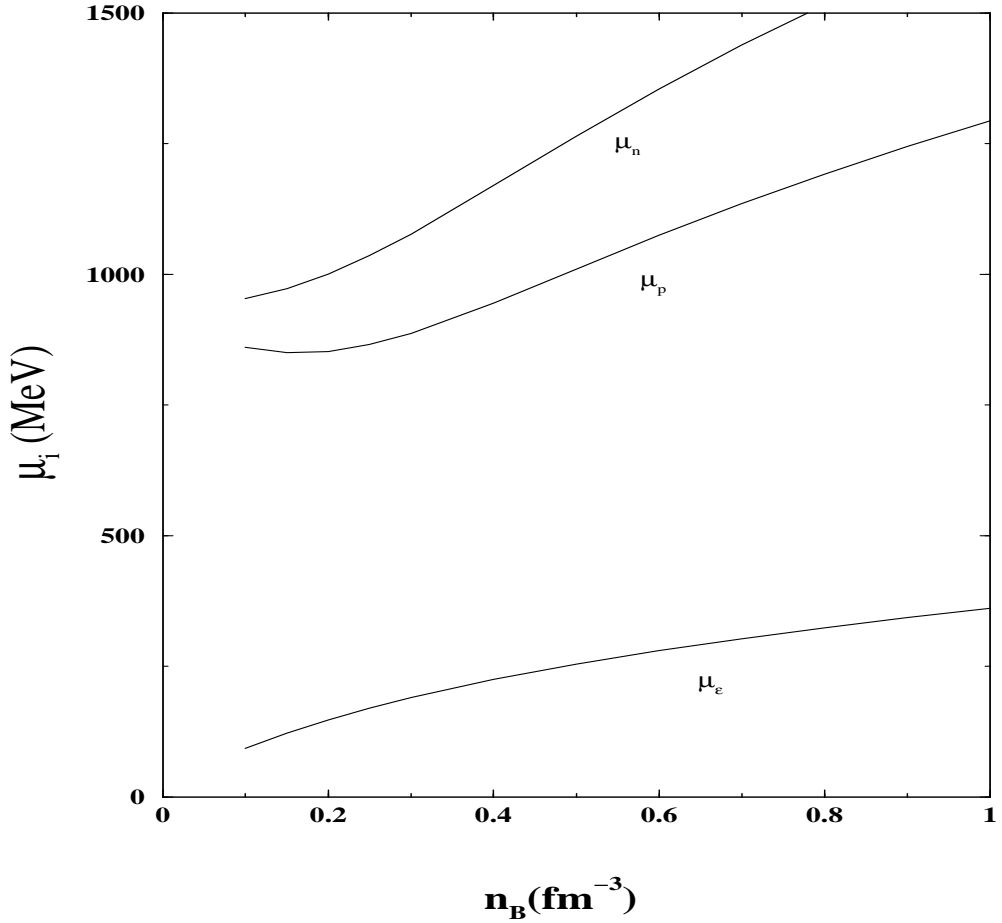


Figure 15: *Chemical potential versus number density in beta-equilibrium at fixed entropy per baryon  $S=1$*

the PNS cools from  $S = 2$  to  $S = 0$ , the maximum mass and radius exhibit a slow decrease. Thus the influence of entropy per baryon or equivalently the temperature, on the structure of PNS is not very sensitive. It is also observed that at finite entropy per baryon e.g.  $S=1$ , the star is proton rich over an extended region of density. The temperature varies slowly in the interior of the star but falls rapidly towards the low density surface region and the maximum temperature of the core of the star for  $S=2$  is about 62 MeV. All these results of PNS are in fair agreement with that obtained in Ref.[2].

### Acknowledgements

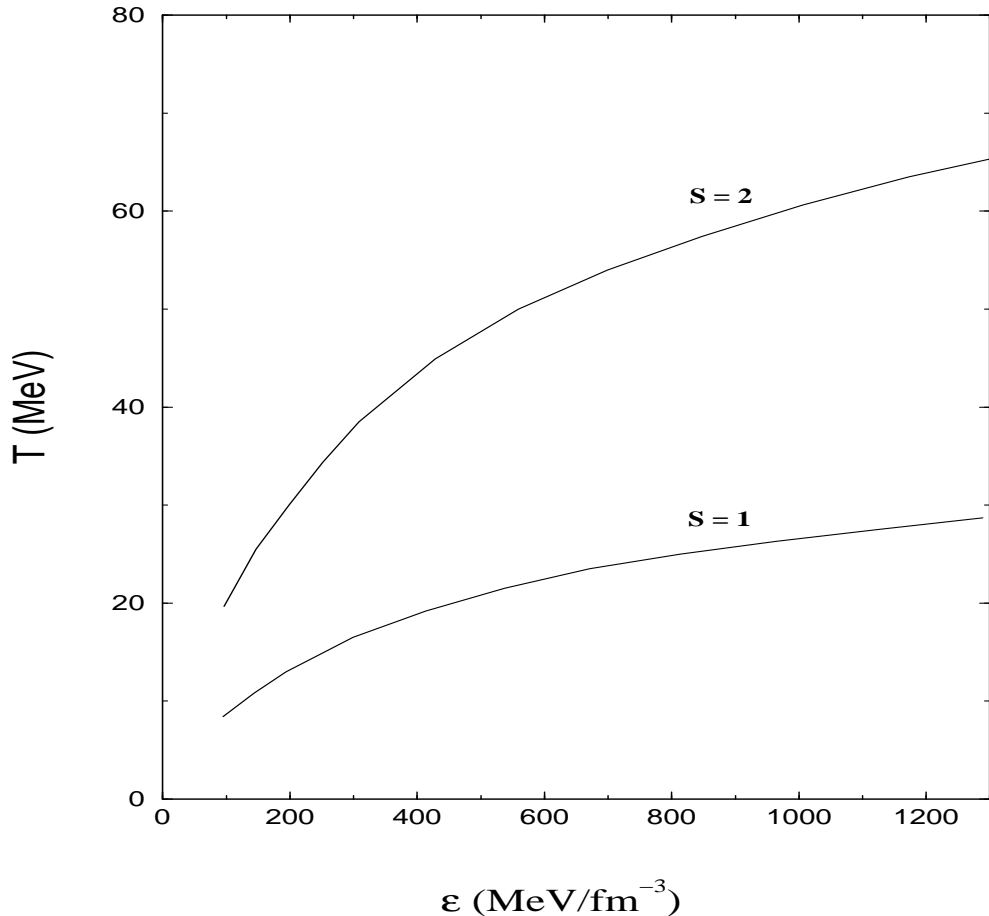


Figure 16: *Temperature versus energy density of proto-neutron star.*

P.K.Jena would like to thank Council of Scientific and Industrial Research, Government of India, for the award of SRF, with financial support under the grant F.No. 9/173 (101)/2000/EMR-I. Help of the Institute of Physics, Bhubaneswar, India, is warmly acknowledged for providing the library and computational facility.

## References

- [1] E. Baron, J. Cooperstein and S. Kahana, *Phy. Rev. Lett.* **55**, 126 (1985); M. Brak, C. Guet and H. B. Hakansson, *Phys.Rep.* **123**, 277 (1985).
- [2] M. Prakash, I. Bombaci, M. Prakash, P. J. Ellis, J. M. Lattimer and R. Knorren, *Phys. Rep.* **280**, 1 (1997).

- [3] W. A. Kupper, G. Wegmann and E. R. Hilf, Ann. phys.(N.Y.) **88**, 454(1974); B. Freedman and V. R. Pandharipande, Nucl. phys. A **361**, 502(1981); H. Jaqaman, A. Z. Mekjian and L. Zamick, Phy. Rev. C **27**, 2782(1983); D. Bandyopadyay, C. Samanta, S. K. Samaddar and J. N. De, Nucl. phys. A **511**, 1(1990).
- [4] H. Q. Song, Z. X. Qian and R. K. Su, Phy. Rev. C **47**, 2001(1993).
- [5] H. Q. Song and R. K. Su, Phys. Lett. B **355**, 179(1995).
- [6] P. Wang, Phy. Rev. C **61**, 054904 (2003).
- [7] H. Müller and B. D. Serot, Phy. Rev. C **52**, 2072(1995).
- [8] P. K. Panda, G. Krein, D. P. Menezes and C. Providencia, Phys. Rev. C **68**, 015201(2003).
- [9] B. D. Serot and J. D. Walecka, Adv. Nucl. Phys. **16** 1 (1986); Int. J. Mod. Phys.E **6**, 515 (1997).
- [10] J. A. Pons, S. Reddy, M. Prakash, J. M. Lattimer and J. A. Miralles, Astrophys.J. **513**, 780(1999).
- [11] G.F.Marranghello, C.A.Z.Vasconcellos, M.Dillig and J.A.D.F.Pacheco, Int. J. Mod. Phys.E **11**, 83(2002).
- [12] P. K. Jena and L. P. Singh, arXiv: nucl-th/0306085.
- [13] P. K. Jena and L. P. Singh, Mod. Phys. Lett. A **17**, 2633 (2002) ; Mod. Phys. Lett. A **18**, 2135 (2003).
- [14] M. Barranco and J. R. Buchler, Phys. Rev.C **22**, 1729(1980).
- [15] N. K. Glendenning, Phys.Rev.D **46**, 1274 (1992).
- [16] J. Theis, G. Graebner, G. Buchwald, J. Maruhn, W. Greiner, H. Stöcker, and J. Polonyi, Phys.Rev.D **28**, 2286 (1983).
- [17] Guo Hua, Liu Bo, M. Di Toro, Phys. Rev. C **62**, 035203(2000).

- [18] M. Malheiro, A. Delfino and C. T. Coelho, Phys. Rev. C **58**, 426(1998).
- [19] R. J. Furnstahl and B. D. Serot, Phys. Rev.C **41**, 262(1990).
- [20] P. K. Panda, A. Mishra, J. M. Eisenberg and W. Greiner Phys. Rev. C **56**, 3134(1997).
- [21] S. Ray, J. Shamanna, T. T. S. Kuo, Phys. Lett. B **392**, 7(1997).
- [22] A. Burrows and J. M. Lattimer, Astrophys.J.**307**, 178(1986).
- [23] J. I. Kapusta, *Finite Temperature Field Theory*. (Cambridge Univ.Press).